PROCEEDINGS OF SCIENCE

Towards the implementation of the photodisintegration interaction in SimProp Sirente

Luciana Andrade Dourado,[a,b,c,*] **Denise Boncioli,**[d,c] **Armando di Matteo,**[e] **Carmelo Evoli,**[a,c] **Sergio Petrera**[a,c] **and Francesco Salamida**[d,c]

[a] *Gran Sasso Science Institute, Viale Francesco Crispi 7, L'Aquila, Italy*
[b] *Dipartimento di Fisica, Università degli Studi di Trento, Via Sommarive 14, Povo, Italy*
[c] *INFN-Laboratori Nazionali del Gran Sasso, Via Giovanni Acitelli 22, L'Aquila, Italy*
[d] *Dipartimento di Scienze Fisiche e Chimiche, Università degli Studi dell'Aquila, Via Vetoio 42, L'Aquila, Italy*
[e] *INFN-Sezione di Torino, Via Pietro Giuria 1, Torino, Italy*

E-mail: luciana.dourado@gssi.it, denise.boncioli@univaq.it, armando.dimatteo@to.infn.it, carmelo.evoli@gssi.it, sergio.petrera@gssi.it, francesco.salamida@univaq.it

The current generation of observatories has confirmed that ultra-high-energy cosmic rays are not composed solely of protons. In particular, analyses of the distributions of shower-maximum depths have revealed an increasing trend in the mass composition of particles with energies above approximately 2 EeV. Given that photodisintegration is the primary interaction for nuclei heavier than protons propagating through intergalactic space, accurately modeling this process is essential for uncovering their astrophysical origins. To address this need, we present revisions to the Monte Carlo propagation code SimProp, emphasizing the implementation of photodisintegration interactions in its upcoming version: SimProp Sirente. Using the latest results from TALYS, a software for nuclear reaction simulations, we compared the total inelastic cross sections with those from one of the current models in SimProp, focusing not only on the cross sections themselves but also on their impact on the energy loss length of the particles. Moreover, we began testing the single-nucleon emission approximation to predict the outgoing nucleus after the interaction occurs, assessing the code's performance in this context and identifying potential improvements in the Sirente version for future applications, such as in-source interactions.

7th International Symposium on Ultra High Energy Cosmic Rays (UHECR2024)
17-21 November 2024
Malargüe, Mendoza, Argentina

*Speaker

© Copyright owned by the author(s) under the terms of the Creative Commons Attribution-NonCommercial-NoDerivatives 4.0 International License (CC BY-NC-ND 4.0).
All rights for text and data mining, AI training, and similar technologies for commercial purposes, are reserved.
ISSN 1824-8039. Published by SISSA Medialab.

PoS(UHECR2024)067

1. Introduction

Three pieces of information that can be obtained from a cosmic ray observatory are the energy spectrum, the distribution of arrival directions, and the particle type identification. For ultra-high-energy cosmic rays (UHECRs, $E > 10^{18}$ eV), the Pierre Auger Observatory (Auger) [1] and the Telescope Array (TA) [2] are the current observatories that perform these measurements indirectly on the ground, using secondary particles from extensive air showers, which develop as a result of the interaction of primary particles at the top of Earth's atmosphere. The mass composition of ultra-high-energy cosmic rays is inferred from the distribution of the maximum shower depth of events, X_{max}, by calculating, for instance, its mean and variance and analyzing their trends with energy. The measurements from the observatories point to a mixed composition for these particles. According to the $\langle X_{\text{max}} \rangle$ measurements from Auger, the mass composition becomes heavier with increasing energy above 2 EeV, which is approximately the energy of the ankle feature.

If ultra-high-energy cosmic rays are not purely composed of protons, it is important to take into account the photodisintegration interaction between these particles and photons in theoretical and phenomenological works, as it is the most significant interaction for nuclei other than protons. This interaction occurs either in the source environment or throughout intergalactic space during propagation. In the case of intergalactic propagation, the most relevant background radiations are the cosmic microwave background (CMB) and the extragalactic background light (EBL). In general, the photodisintegration reaction is written as

$$X(A, Z) + \gamma \rightarrow X'(A', Z') + \ldots, \tag{1}$$

where the original nucleus $X(A, Z)$ interacts with a photon γ, resulting in another nucleus $X'(A', Z')$ being created and the emission of one or more nuclei at the end, represented by the three dots above. The most important channels, which are the most probable ones to happen, are the one-particle emission either of a nucleon, which is a proton or a neutron, or an alpha particle. While the probability of this interaction to take place depends on the total inelastic cross section of the interaction, the probability of a specific channel occurring depends on the exclusive cross section for that channel, which may involve the emission of one or more particles. Although several experiments [3, 4] have been conducted to determine the cross sections of some nuclear reactions, measurements for some nuclei are still lacking [5]. In the absence of cross-section data for all nuclei, other resources for obtaining such information are software packages used in the field of nuclear physics, such as TALYS [6] and FLUKA [7, 8].

Therefore, it is crucial to model the photodisintegration interaction, which includes its cross sections and channels. This is done, for instance, in propagation codes, such as CRPropa [9], PriNCe [10], and SimProp [11]. In particular, SimProp is a Monte Carlo code for the propagation of ultra-high-energy cosmic rays, first published in 2012. While the latest version, SimProp v2r4, is seven years old and includes four models for the photodisintegration interaction, the next version, called SimProp Sirente, is under development and will feature an updated photodisintegration model.

This work moves towards the implementation of the photodisintegration interaction in SimProp Sirente. We aim to compare one of the photodisintegration models from SimProp v2r4 with the most up-to-date cross-section data from TALYS, focusing particularly on the energy loss length

PoS(UHECR2024)067

derived from these cross sections and the new nuclei produced after the interactions occur. This proceeding is structured as follows. In Section 2, we describe the photodisintegration model from SimProp v2r4 that were used for comparisons. In Section 3, we present the cross sections derived from measurements, TALYS, and SimProp v2r4 for two nuclei. We also display the interaction lengths for several nuclei and plot the relative differences between the two models. In Section 4, we use the same model from SimProp v2r4 to compare the differences in the nuclei produced after the interaction with those predicted by TALYS. In Section 5, we outline our conclusions.

2. Photodisintegration implementation in SimProp v2r4

There are four models for photodisintegration implemented in SimProp v2r4, as referenced in [11]. In particular, the fourth model is structured around the emission of either a nucleon or an alpha particle, which are the most significant channels for photodisintegration. The interaction cross section was parameterized with a fit of the cross sections from TALYS-1.6[1], using a Gaussian function around the resonance of the cross section, followed by a constant function thereafter:

$$\sigma_i(\epsilon') = \begin{cases} h_i^1 \exp\left[-\frac{(\epsilon'-x_i^1)^2}{w_i^1}\right], & t_i < \epsilon' < \epsilon_1, \quad i = N, \alpha, \\ c_i, & \epsilon_1 < \epsilon' < \epsilon_{\max}, \quad i = N, \alpha, \end{cases} \tag{2}$$

where ϵ' is the energy of the photon in the nucleus rest frame, and h_i^1, x_i^2, w_i^1, c_i, t_i, ϵ_1, and $\epsilon_{\max}$ are constants from the parameterization provided in the file `xsect_Gauss2_TALYS-restored.txt`, included in the SimProp v2r4 download package[2]. Furthermore, the index i indicates whether the values correspond to the emission of a nucleon N or an alpha particle α. The cross-section values are available for several nuclei, ranging from deuterium to iron-56, in terms of mass composition.

This fourth photodisintegration model from SimProp v2r4 is the one used for the analyses in this work. This specific model was chosen because it is the latest version available in SimProp and is commonly used in works, such as the combined fit analyses by the Pierre Auger Collaboration [12]. From now on, we will refer to this model simply as “SimProp v2r4” model.

3. Total inelastic cross sections and energy loss lengths

Using available measurements of cross sections from the Experimental Nuclear Reaction Data (EXFOR) library [13], which contains an extensive compilation of experimental nuclear reaction data, we compared measured cross sections for the photodisintegration interaction of some nuclei with the cross sections from SimProp v2r4 model and the latest TALYS data: TALYS-2.0[3]. The tables with the TALYS cross sections are available in TENDL [14], which is a nuclear data library that provides the outputs of the TALYS nuclear model code system for direct use. Therefore, we used TENDL-2023 tables, which contain the TALYS-2.0 data, and we will refer to these cross sections as “TENDL-2023" in the plots.

Figure 1 presents the total inelastic cross section for oxygen-16 and aluminum-27. The measurements for oxygen-16, as reported in EXFOR, were obtained by Wyckoff et al. (1965) [15],

[1] Available at https://nds.iaea.org/talys/.
[2] Available at https://github.com/SimProp/SimProp-v2r4.
[3] Available at https://nds.iaea.org/talys/.

PoS(UHECR2024)067

Bezić et al. (1969) [16], and Ahrens et al. (1972). For aluminum-27, the measurements were conducted by Wyckoff et al. (1965) [15], Ahrens et al. (1972), Ahrens et al. (1975) [17], and Ahrens (1985) [18]. Comparing these distinct nuclei reveals that the cross section increases with the mass number of the isotope, A. In the case of SimProp v2r4, we summed the two channels of the emission of a nucleon and alpha particle to obtain the total cross section.

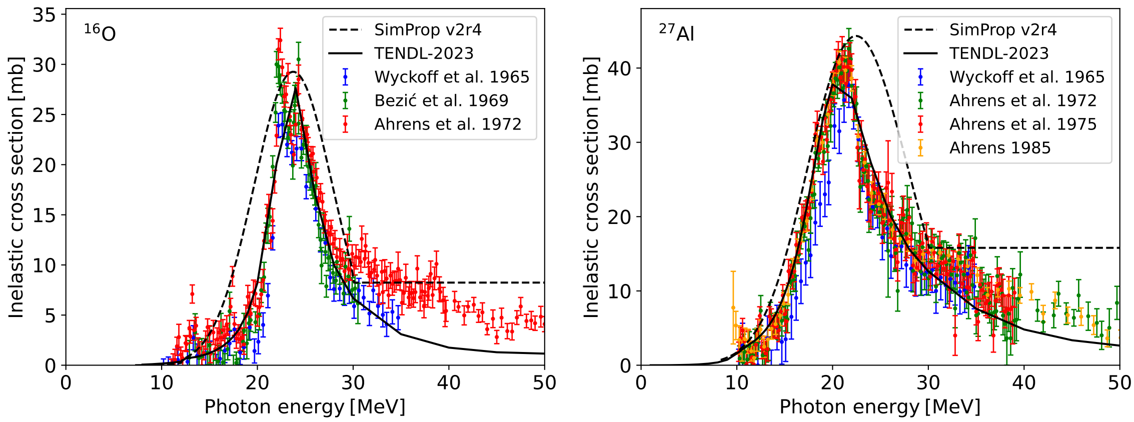

Figure 1: Total inelastic cross sections as functions of the photon energy in the nucleus rest frame for oxygen-16 and aluminium-27, shown in the *left* and *right panels*, respectively.

Although some differences can be observed between the total cross sections from the measurements, TENDL-2023, and the SimProp v2r4 model, what matters in terms of the total inelastic cross section is how these differences affect the interaction length of ultra-high-energy cosmic rays. This interaction length is the key value used in the propagation codes of ultra-high-energy cosmic rays to determine whether an interaction will take place or not. The expression for the energy loss length, defined as the interaction length multiplied by the nucleus' mass number A, as a function of the nucleus's Lorentz factor Γ, is given by:

$$\lambda_A(\Gamma) = A \left[\frac{1}{2\Gamma^2} \int_{\epsilon_{\rm th}}^{\infty} d\epsilon' \epsilon' \sigma_A(\epsilon') \int_{\frac{\epsilon'}{2\Gamma}}^{\infty} d\epsilon \frac{n_\gamma(\epsilon)}{\epsilon^2} \right]^{-1}, \tag{3}$$

where c is the speed of light, σ_A is the total inelastic cross section of the interaction, where the subscript A refers to the original nucleus, not the reaction channel as in Equation (2), $\epsilon_{\rm th}$ is the energy threshold of the interaction, and n_γ is the density distribution of the radiation field under consideration. Moreover, ϵ' and ϵ are the photon energies in the nucleus rest frame and the laboratory frame, respectively.

The left panel of Figure 2 shows the energy loss length of distinct nuclei in the presence of only the CMB as the radiation background as a function of the base-10 logarithm of the nucleus energy. The results are based on cross-section values from both TENDL-2023 and SimProp v2r4. We can observe some differences between the two models. To further illustrate this, we also plotted the percentage difference between the two models, which can be seen in the right panel of Figure 2. The relative differences were built as the absolute difference between interaction length derived from the two models of cross section, TENDL-2023 and SimProp v2r4, divided by values of the interaction length of the TENDL-2023. Moreover, it is shown in the Figure 2 only the values of

PoS(UHECR2024)067

the differences where the interaction length of TENDL-2023 is below the adiabatic energy loss length. After the energy threshold, where the interaction length decreases, the differences between the models become more pronounced, although this occurs at very high energy values. Below the energy of $10^{20.5}$ eV, which is about the energy of the second most energetic event ever detected on Earth [19], the highest relative difference is about 40%, which was for oxygen-16.

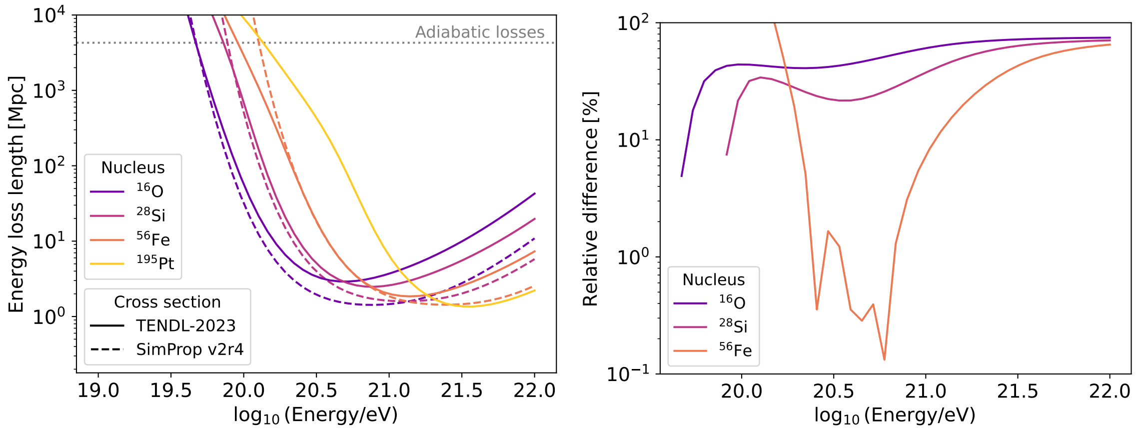

Figure 2: Energy loss length as a function of the base-10 logarithm of the particle energy using cross sections from TENDL-2023 (*solid lines*) and SimProp v2r4 (*dashed lines*) in the *left panel*, and their relative difference in the *right panel*. Four distinct nuclei are shown: oxygen (^{16}O, *purple curves*), silicon (^{28}Si, *pink curves*), iron (^{56}Fe, *coral curves*), and platinum (^{195}Pt, *yellow curves*). The dotted gray line in the *left panel* represents the interaction length for adiabatic losses.

The energy loss length for an ultra-heavy nucleus ($A > 56$), platinum-197, which was not included in the current version of SimProp, was also plotted in Figure 2. By observing the behavior of the energy loss length as a function of mass number at a fixed energy within the range of the highest-energy events, it is expected that heavier particles originate from larger distances, since the energy loss length decreases with increasing energy in this energy range. This is important, for instance, for horizon studies, which have varying definitions in the literature [20–22], but broadly refer to the maximum distance of the source for an event.

4. Testing the single-nucleon emission approximation

If photodisintegration occurs, the identity of the nucleus in the final state is determined by the exclusive cross section of each reaction channel. The potential differences between the expected final-state composition predicted by TALYS-2.0 and the one obtained under the single-nucleon approximation implemented in SimProp v2r4 is an important aspect to be investigated. As described in Section 2, the SimProp v2r4 model considers only the emission of a single nucleon or an alpha particle, while TALYS-2.0 also accounts for multi-particle emission processes.

For illustration, Figure 3 shows the mean natural logarithm of the mass number of the residual nucleus as a function of photon energy in the nuclear rest frame, considering oxygen-16 and aluminium-27 as the primary species. The predictions of SimProp v2r4 and TALYS-2.0 exhibit good agreement up to photon energies of approximately 20 MeV, but discrepancies increase at

PoS(UHECR2024)067

higher energies. In this high-energy regime, the mean value of $\ln A$ from TALYS-2.0 decreases due to the growing probability of multi-particle emission channels, which lead to lighter final-state nuclei on average.

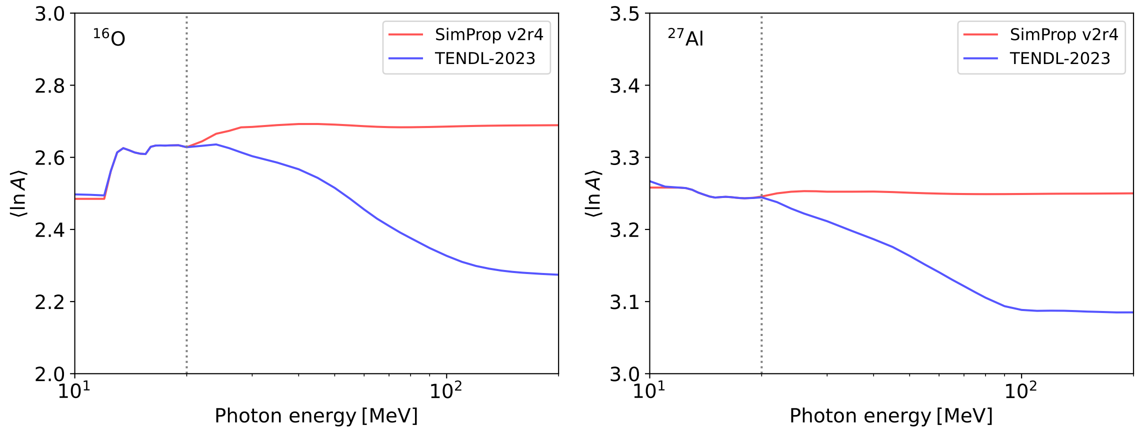

Figure 3: Mean value of the natural logarithm of the mass number of the new nucleus created after a photodisintegration interaction, as a function of the photon energy in the nucleus rest frame, for oxygen-16 (*left panel*) and aluminium-27 (*right panel*) as original nuclei. The blue line represents results considering all possible exclusive channels from TENDL-2023, while the red line shows results for the single-nucleon approximation using SimProp v2r4.

For the CMB, which is the most significant radiation field for the propagation of ultra-high-energy cosmic rays, the photon energy at the peak of the distribution is about 2.33×10^{-4} eV in the laboratory frame. This means that for this photon to be boosted to 20 MeV, it requires an interaction with a nucleus that has a Lorentz factor around 10^{10}. In the case of an iron nucleus, this implies an energy of approximately 6×10^{20} eV, which exceeds the maximum energy observed in cosmic ray events. Therefore, the energy range relevant for ultra-high-energy cosmic rays remains relatively unaffected in this situation. A similar reasoning can be made for the EBL, characterized by higher photon energies compared to the CMB, causing the energy of the ultra-high-energy cosmic rays necessary for photodisintegration to shift towards lower energies.

5. Conclusions

A new release of the SimProp code is currently under development to meet the demanding requirements of next-generation ultra-high-energy cosmic ray experiments. One of the key improvements in this update is the revision of the photodisintegration model, which is crucial for accurately simulating the composition of UHECRs. To achieve this, we began by comparing one of the SimProp v2r4 models with recent TALYS cross sections, particularly focusing on the energy loss length of particles and testing the single-nucleon emission approximation.

For SimProp Sirente, we aim to use the cross sections for stable nuclei, including ultra-heavy nuclei, not only from TALYS but also from FLUKA, to compute interaction length tables that will determine whether an interaction takes place in the simulations. The next steps regarding this point involve comparing the total inelastic cross sections for stable nuclei from TALYS-2.0

PoS(UHECR2024)067

against experimental measurements, assessing whether any modifications are necessary to refine the photodisintegration model. For the outgoing nucleus after photodisintegration, we plan to extend the model by incorporating some multi-particle emission channels to enhance the accuracy of SimProp Sirente and provide a more realistic description of nuclear fragmentation processes beyond the single-particle approximation, specially for future applications such as modeling in-source interactions. The specific channels to be selected for the new model are yet to be decided, and validation tests, such as those outlined in [5], can be performed to ensure that the model achieves the necessary precision in predicting the production of new nuclei.

6. Acknowledgments

This publication was produced while attending the PhD program in PhD in Space Science and Technology at the University of Trento, Cycle XXXIX, with the support of a scholarship financed by the Ministerial Decree no. 118 of 2nd March 2023, based on the NRRP - funded by the European Union - NextGenerationEU - Mission 4 "Education and Research", Component 1 "Enhancement of the offer of educational services: from nurseries to universities" - Investment 4.1 "Extension of the number of research doctorates and innovative doctorates for public administration and cultural heritage" - CUP E66E23000110001.

References

[1] Pierre Auger collaboration, *The Pierre Auger Cosmic Ray Observatory*, *Nucl. Instrum. Meth. A* **798** (2015) 172 [1502.01323].

[2] H. Kawai, S. Yoshida, H. Yoshii, K. Tanaka, F. Cohen, M. Fukushima et al., *Telescope Array Experiment*, *Nuclear Physics B Proceedings Supplements* **175** (2008) 221.

[3] E. Kido, T. Inakura, M. Kimura, N. Kobayashi, S. Nagataki, N. Shimizu et al., *Evaluations of uncertainties in simulations of propagation of ultrahigh-energy cosmic-ray nuclei derived from microscopic nuclear models*, *Astropart. Phys.* **152** (2023) 102866 [2206.03447].

[4] PANDORA collaboration, *PANDORA Project for the study of photonuclear reactions below* $A = 60$, *Eur. Phys. J. A* **59** (2023) 208 [2211.03986].

[5] D. Boncioli, A. Fedynitch and W. Winter, *Nuclear Physics Meets the Sources of the Ultra-High Energy Cosmic Rays*, *Scientific Reports* **7** (2017) 4882 [1607.07989].

[6] A.J. Koning and D. Rochman, *Modern Nuclear Data Evaluation with the TALYS Code System*, *Nuclear Data Sheets* **113** (2012) 2841.

[7] FLUKA collaboration, *The FLUKA code: Overview and new developments*, *EPJ Nuclear Sci. Technol.* **10** (2024) .

[8] M.N. Mazziotta, F. Cerutti, A. Ferrari, D. Gaggero, F. Loparco and P.R. Sala, *Production of secondary particles and nuclei in cosmic rays collisions with the interstellar gas using the FLUKA code*, *Astroparticle Physics* **81** (2016) 21 [1510.04623].

PoS(UHECR2024)067

[9] R. Alves Batista, J. Becker Tjus, J. Dörner, A. Dundovic, B. Eichmann, A. Frie et al., *CRPropa 3.2 - an advanced framework for high-energy particle propagation in extragalactic and galactic spaces*, J. Cosmology Astropart. Phys. **2022** (2022) 035 [2208.00107].

[10] J. Heinze, A. Fedynitch, D. Boncioli and W. Winter, *A New View on Auger Data and Cosmogenic Neutrinos in Light of Different Nuclear Disintegration and Air-shower Models*, ApJ **873** (2019) 88 [1901.03338].

[11] R. Aloisio, D. Boncioli, A. Di Matteo, A.F. Grillo, S. Petrera and F. Salamida, *SimProp v2r4: Monte Carlo simulation code for UHECR propagation*, *JCAP* **11** (2017) 009 [1705.03729].

[12] Pierre Auger collaboration, *Combined fit of spectrum and composition data as measured by the Pierre Auger Observatory*, *JCAP* **04** (2017) 038 [1612.07155].

[13] N. Otuka, E. Dupont, V. Semkova, B. Pritychenko, A.I. Blokhin, M. Aikawa et al., *Towards a More Complete and Accurate Experimental Nuclear Reaction Data Library (EXFOR): International Collaboration Between Nuclear Reaction Data Centres (NRDC)*, *Nuclear Data Sheets* **120** (2014) 272 [2002.07114].

[14] A.J. Koning, D. Rochman, J.C. Sublet, N. Dzysiuk, M. Fleming and S. van der Marck, *TENDL: Complete Nuclear Data Library for Innovative Nuclear Science and Technology*, *Nuclear Data Sheets* **155** (2019) 1.

[15] J.M. Wyckoff, B. Ziegler, H.W. Koch and R. Uhlig, *Total Photonuclear Cross Sections for Low Atomic Number Elements*, *Physical Review* **137** (1965) 576.

[16] N. Bezić, D. Brajnik, D. Jamnik and G. Kernel, *Total photonuclear cross sections for ^{12}C, ^{14}N, ^{16}O and ^{19}F in the region of the giant resonance*, Nucl. Phys. A **128** (1969) 426.

[17] J. Ahrens, H. Borchert, K.H. Czock, H.B. Eppler, H. Gimm, H. Gundrum et al., *Total nuclear photon absorption cross sections for some light elements*, Nucl. Phys. A **251** (1975) 479.

[18] J. Ahrens, *The total absorption of photons by nuclei*, Nucl. Phys. A **446** (1985) 229.

[19] Telescope Array collaboration, *An extremely energetic cosmic ray observed by a surface detector array*, *Science* **382** (2023) abo5095 [2311.14231].

[20] D. Harari, S. Mollerach and E. Roulet, *On the ultrahigh energy cosmic ray horizon*, J. Cosmology Astropart. Phys. **2006** (2006) 012 [astro-ph/0609294].

[21] N. Globus, A. Fedynitch and R.D. Blandford, *Treasure Maps for Detections of Extreme Energy Cosmic Rays*, ApJ **945** (2023) 12 [2210.15885].

[22] M. Unger and G.R. Farrar, *Where Did the Amaterasu Particle Come From?*, ApJ **962** (2024) L5 [2312.13273].

PoS(UHECR2024)067